Adsorption of Cu, Pd, and Cs Atoms on Regular and Defect Sites of the SiO_2 Surface

Nuria Lopez,[†,‡] Francesc Illas,[‡] and Gianfranco Pacchioni*[,†]

Contribution from the Istituto Nazionale di Fisica della Materia, Dipartimento di Scienza dei Materiali, Università di Milano, via Emanueli, 15, 20126 Milano, Italy, and Departament de Quimica Fisica, Universitat de Barcelona, Marti i Franques 1, 08028 Barcelona, Spain

Received May 20, 1998. Revised Manuscript Received September 4, 1998

Abstract: The interaction of isolated Cu, Pd, and Cs atoms on regular and defect sites of the SiO_2 surface has been studied with cluster models. Hartree−Fock, density functional theory, and multireference configuration interaction methods have been used to characterize the bonding of the metal atoms at the following sites: bridging oxygens at the regular surface, ≡Si−O−Si≡, Si singly occupied sp^3 dangling bonds (E′ centers), ≡Si•, nonbridging oxygen centers, ≡Si−O•, and neutral oxygen vacancies, ≡Si−Si≡. The bonding with the nondefective sites of the surface is very weak, <0.2 eV. Sticking of the atoms occurs only at the defect sites with adsorption energies ranging from 1 to 3 eV. Several spectral signatures of the bond at the silica defects have been considered: core level shifts, impurity levels in the band gap, and optical transitions.

1. Introduction

The metal/oxide interface is an extremely important aspect of surface science related to a variety of technological applications, from microelectronics to coating and protection of metals, from nonlinear optics phenomena to colloid chemistry, catalysis, and gas sensor applications. However, it is difficult to study oxides (supports) using surface science techniques because their nonconductive and brittle nature causes experimental difficulties related to sample charging and heating. An approach that has been used to facilitate the study of oxides and metal−support interactions is to prepare oxide thin films on a metal surface.[1,2] Several metal−support systems of chemical interest have been addressed using this approach.[1−3] Another approach is the controlled dispersion from aqueous solution of metal complexes onto the support.[4] Theoretical studies, in particular if performed with first-principle approaches, can provide a useful complement to experiment for the understanding of the microscopic aspects of the interaction. However, the quantum-mechanical description of the interaction of metal atoms or clusters with the surface of oxide materials is still at the very beginning.[5] In fact, only relatively few first-principle theoretical studies have been performed on this topic so far.[6−12] One of the reasons, beside the complexity of the systems to investigate, is the lack of accurate experimental information about the structural aspects of the metal/oxide interface. Even a simple question like which is the preferred adsorption site for an Ag atom on a simple surface such as that of MgO has been answered experimentally only very recently.[13] In the past few years, however, experimental studies on well-defined oxide surfaces have been reported in the literature, facilitating the direct comparison of observations with theoretical predictions.[14−18] In absence of experimental input, the atomistic aspects of the metal/oxide interaction have to be assumed on the basis of simple models or chemical intuition. Another critical aspect of the quantum-mechanical simulation of these systems is the great variety of supporting oxides, from very ionic, like MgO, to largely covalent, like SiO_2, or intermediate, e.g. TiO_2 or Al_2O_3. Finally, even when the geometrical and electronic structure of the oxide surface is sufficiently well characterized, the early stages of the deposition often involve defects and surface irregularities and not the regular full-coordinated sites.

In this study, we report the first quantum-mechanical study of the interaction of metal atoms (Cu, Pd, and Cs) with regular and defect sites of the dehydroxilated SiO_2 surface. We have performed ab initio Hartree−Fock (HF) and gradient-corrected density functional theory (DFT) cluster calculations on models of the SiO_2 surface sites. The choice of studying Cu, Pd, and Cs on SiO_2 is due to the existence of experimental data[18−22] on

[†] Università di Milano.
[‡] Universitat de Barcelona.

(1) Vurens, G. H.; Salmeron, M.; Somorjai, G. A. *Prog. Surf. Sci.* **1989**, *32*, 333.
(2) Lambert, R. M., Pacchioni, G., Eds. *Chemisorption and Reactivity on Supported Clusters and Thin Films*; NATO ASI Series E, Vol. 331; Kluwer: Dordrecht, The Netherlands, 1997; p 353.
(3) Levin, M. E.; Williams, K. J.; Salmeron, M.; Bell, A. T.; Somorjai, G. A. *Surf. Sci.* **1988**, *195*, 341.
(4) Carriat, J. Y.; Che, M.; Kermarec, M.; Verdaguer, M.; Michalowicz, A. *J. Am. Chem. Soc.* **1998**, *120*, 2059.
(5) Rösch, N.; Pacchioni, G. In ref 2, p 353.
(6) Pacchioni, G.; Rösch, N. *Surf. Sci.* **1994**, *306*, 169.
(7) Pacchioni, G.; Rösch, N. *J. Chem. Phys.* **1996**, *104*, 7329.
(8) Yudanov, I.; Pacchioni, G.; Neyman, K.; Rösch, N. *J. Phys. Chem. B* **1997**, *101*, 2786.
(9) Li, C.; Wu, R.; Freeman, A. J.; Fu, C. L. *Phys. Rev. B* **1993**, *48*, 8317.
(10) Li, Y.; Landgreth, D. C.; Pederson, M. R. *Phys. Rev. B* **1995**, *52*, 6067.
(11) Stirling, A.; Gunji, I.; Endou, A.; Oumi, Y.; Kubo, M.; Miyamoto, A. *J. Chem. Soc., Faraday Trans.* **1997**, *93*, 1175.
(12) Lopez, N.; Illas, F. *J. Phys. Chem. B* **1998**, *102*, 1430.
(13) Flank, A. M.; Delaunay, R.; Lagarde, P.; Pompa, M.; Jupille, J. *Phys. Rev. B* **1996,** *53*, R1737.
(14) Freund, H. J. *Angew. Chem.* **1997**, *109*, 444.
(15) Campbell, C. T. *Surf. Sci. Rep.* **1997,** *27*, 1.
(16) Gunter, P. L. J.; Niemantsverdriet, J. W.; Ribeiro, F. H.; Somorjai, G. A. *Catal. Rev.-Sci. Eng.* **1997**, *39*, 77.
(17) Sauer, J.; Ugliengo, P.; Garrone, E.; Saunders: V. R. *Chem. Rev.* **1994**, *94*, 2095.
(18) Xu, X.; Goodman, D. W. *Appl. Phys. Lett.* **1992**, *61*, 1799.
(19) Xu, X.; He, W.; Goodman, D. W. *Surf. Sci.* **1993**, *284*, 103.
(20) Zhou, J. B.; Lu, H. C.; Gustafsson, T.; Garfunkel, E. *Surf. Sci. Lett.* **1993**, *293*, L887.

10.1021/ja981753c CCC: $18.00
Published on Web 01/13/1999

these systems but also to our recent studies on the electronic structure and spectral properties of point defects in bulk silica.[23−25] The adsorption sites considered are (1) regular bridging oxygens at the deydroxilated surface, ≡Si−O−Si≡; (2) E′ defect centers corresponding to a Si singly occupied sp^3 dangling bond, ≡Si•; (3) nonbridging oxygen (NBO), ≡Si−O•, centers; (4) neutral oxygen vacancies, ≡Si−Si≡ or V_O. While the E′ and NBO defects are paramagnetic and detectable by EPR spectroscopy, the neutral oxygen vacancy is EPR silent and can only be detected with other techniques. All of these defects have attracted great interest in the past 20 years because of their role in the degradation of Si/SiO_2 interfaces in microelectronics devices and in the absorption of light in optical fibers.[26] Literally hundreds of papers have been devoted to this problem. Very similar defects are present in the bulk of amorphous silica and α-quartz[26] and on the surface of mechanically activated silica,[27,28] of SiO_2 thin films,[29] and of UHV cleaved α-quartz single crystals.[30,31] The fingerprints of the presence of these centers on the surface are typical EPR signals and hyperfine coupling constants of the unpaired electron with the ^{29}Si and ^{17}O nuclear spins but also characteristic absorption bands at 5.8 eV (E′), 2 eV (NBO), and 7.6 eV (V_O) in the optical spectra of the material.[25,26] It has been suggested that these defect centers are the primary cause of the interface bond formation.[19,20,22] The scope of this paper is to elucidate their role in the early stages of the deposition of metal atoms on the silica surface. Since many catalysts consist of small particles on high-surface-area powders of SiO_2 or Al_2O_3, the understanding at a microscopic level of the metal−oxide interaction, in particular at the defect sites, is the essential prerequisite for the understanding of the catalytic activity.

2. Computational Approach

To describe the regular oxygen sites as well as some point defects at the surface of SiO_2 we used cluster models whose structures were derived from that of α-quartz.[32] The cluster broken bonds have been saturated by H atoms placed at 0.98 Å from the O atoms along the O−Si bond directions of the perfect crystal. The H atoms have been kept fixed during the geometrical optimization to provide a simple representation of the mechanical embedding of the solid matrix. In a separate study[33] we considered larger clusters as well as a combined quantum-mechanical molecular mechanics, QM+MM, approach for the specific case of Cu adsorption. We found that the small clusters adopted in this study give results very similar to those of larger clusters or a more sophisticated QM+MM approach. The reason is that the bonding of metal atoms at these sites is very local and does depend on the nearest neighbors only.

The regular ≡Si−O−Si≡ site of the silica surface has been represented by a $(HO)_3Si-O-Si(OH)_3$ cluster (Figure 1a). The

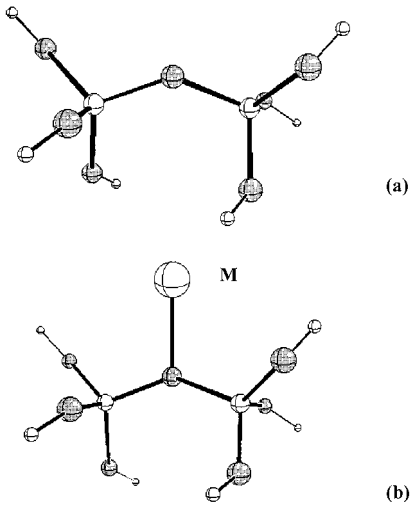

Figure 1. Cluster models of: (a) a two-coordinated bridging oxygen, ≡Si−O−Si≡, at the nondefective silica surface; (b) a metal atom (Cu, Pd, Cs) adsorbed on-top of the bridging oxygen.

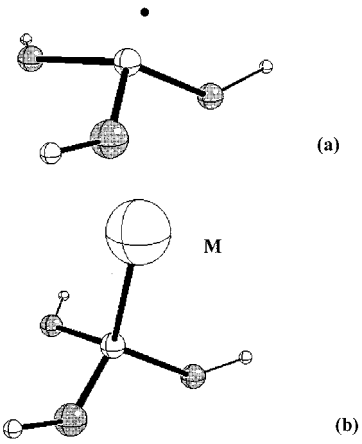

Figure 2. Cluster models of (a) a E'_S center, ≡Si•, at the silica surface and (b) a metal atom (Cu, Pd, Cs) adsorbed on the E'_S center, ≡Si−M.

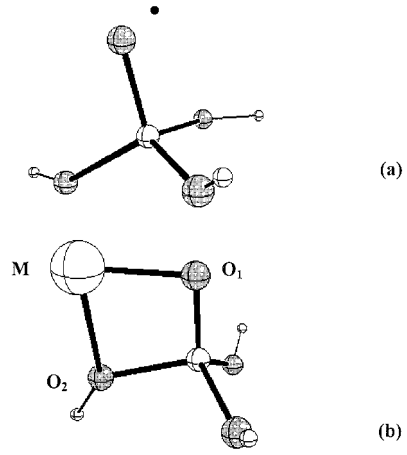

Figure 3. One-tetrahedron, 1-T, cluster models of (a) a nonbridging oxygen (NBO) center, ≡Si−O•, at the silica surface and (b) a metal atom (Cu, Pd, Cs) adsorbed on the NBO center.

E′ center, ≡Si•, was described by a $(HO)_3Si^•$ unit (Figure 2a). The clusters used to model the ≡Si−O• group are $(HO)_3Si-O^•$ (Figure 3a) and $(HO)_3Si-O-(HO)_2Si-O^•$ (Figure 4a). The two clusters contain one and two tetrahedral Si atoms, respectively, and are thereafter denoted for brevity as 1-T and 2-T. The two clusters give somewhat different results for reasons that will

(21) Zhou, J. B.; Gustafsson, T.; Garfunkel, E. *Surf. Sci.***1997**, *372*, 21.
(22) Brause, M.; Ochs, D.; Günster, J.; Mayer, T.; Braun, B.; Puchin, V.; Maus-Friedrichs, W.; Kempter, V. *Surf. Sci.* **1997,** *383*, 216.
(23) Pacchioni, G.; Ieranò, G. *Phys. Rev. B* **1997**, *56*, 7304.
(24) Pacchioni, G.; Ieranò, G. *Phys. Rev. Lett.* **1997**, *79*, 753.
(25) Pacchioni, G.; Ieranò, G. *Phys. Rev. B* **1998**, *57*, 818.
(26) Arndt, J., Devine, R., Revesz, A., Eds. *The Physics and Technology of Amorphous SiO2*; Plenum: New York, 1988.
(27) Radtsig, V. A. *Chem. Phys. Rep.* **1995**, *14*, 1206.
(28) Hochstrasser, G.; Antonini, J. F. *Surf. Sci.* **1972**, *32*, 644.
(29) Xu, X.; Goodman, D. W. *Appl. Phys. Lett.* **1992**, *61*, 774.
(30) Bart, F.; Gautier, M.; Jollet, F.; Durand, J. P. *Surf. Sci.* **1994**, *306*, 342.
(31) Bart, F.; Gautier, M.; Durand, J. P.; Henriot, M. *Surf. Sci.* **1992**, *274*, 317.
(32) Le Page, Y.; Calvert, L. D.; Gabe, E. J. *J. Phys. Chem. Solids* **1980**, *41*, 721.
(33) Lopez, N.; Pacchioni, G.; Maseras, F.; Illas, F. *Chem. Phys. Lett.* **1998**, *294*, 611.

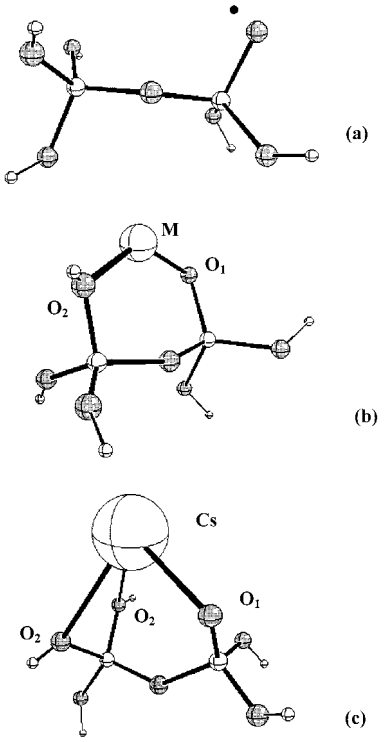

Figure 4. Two-tetrahedra, 2-T, cluster models of (a) a nonbridging oxygen (NBO) defect center, ≡Si−O•, at the silica surface, (b) a Cu or Pd atom adsorbed on the NBO center and (c) a Cs atom adsorbed on a NBO center.

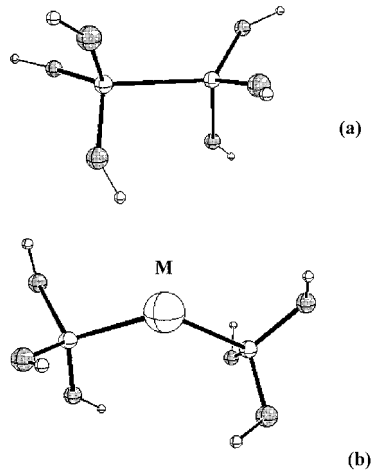

Figure 5. Cluster models of (a) a neutral oxygen vacancy center, ≡Si−Si≡, at the silica surface and (b) a Cu or Pd atom adsorbed on the neutral oxygen vacancy, ≡Si−M−Si≡.

be clarified below. Finally, a $(HO)_3Si-Si(OH)_3$ cluster (Figure 5a) was used to represent the neutral oxygen vacancy on the silica surface. Full geometry optimizations have been performed by means of analytical gradients of the total energy with the constraint of fixed embedding H atoms.

The cluster wave functions have been computed at the restricted HF or restricted open HF levels. Correlation effects have been introduced by performing DFT calculations (spin polarized for open shell cases) using the Becke's three-parameter hybrid nonlocal exchange functional[34] combined with the Lee−Yang−Parr gradient-corrected correlation functional[35] (B3LYP). The basis sets used are 6-31G* [36] on Si and on the O atom directly interacting with the metal and 6-31G, 3-21G, and 3-21G on the other Si, O, and H atoms, respectively.[37] For Cu we used an all-electron (AE) basis set from Whatcher, [14s11p6d/8s6p4d].[38] Pd and Cs have been treated with a relativistic effective core potential (ECP), which includes explicitly in the valence the $4s^24p^64d^{10}$ electrons of Pd[39] and the $5s^25p^66s^1$ electrons of Cs[40] (small core ECP). The Pd and Cs basis sets are [5s5p4d] (uncontracted) and [8s6p/3s3p], respectively.[39,40] All of the binding energies have been corrected by the full counterpoise basis set superposition error (BSSE) procedure.[41] In most of the systems studied the BSSE is rather large. This is because of the use of a small basis set on the atoms of the cluster not directly interacting with the adsorbed metal atom. The counterpoise method is particularly suited for systems which do not undergo a strong geometrical relaxation after bonding formation. When the geometry of the two interacting fragments changes slightly, the Emsley procedure can be adopted.[42] In this case the BSSE is determined for the optimal final structure and then added to the interaction energy computed with respect to the separated fragments in their equilibrium geometries. However, in some cases discussed here, the geometry relaxation is so large that the procedure does not provide a realistic estimate of the BSSE but only an upper bound. For this reason we report in the tables both final and BSSE-corrected energies (B3LYP results only).

Core level ionization potentials (IPs) have been analyzed to gain information about the interaction modes of the adsorbed atoms. Core level binding energies have been considered based on the Koopmans' theorem, $IP = -\epsilon_i$, where ϵ_i is the eigenvalue corresponding to a given core level. In HF theory, this corresponds to the initial state IP of the core orbital and does not include final state relaxation following the core hole formation. In DFT, we have taken the negative Kohn−Sham eigenvalues as a measure of the corresponding IP. This procedure is not fully justified by DF theory, but experience shows that it provides an acceptable, and often a very good approximation to the final state core level binding energies.[43] Binding energy shifts, ΔIP, have been computed with respect to the free surface site, with no metal adsorbed, or to the free metal atoms. For O, Si, and Cu atoms, where an AE basis set was used, we have considered the 1s (O) and 2p (Si and Cu) core levels which are usually measured in XPS experiments. For Pd and Cs, where an ECP was used, we have considered the semi-core 4s and 5s levels, respectively.

One important experimental way to characterize the presence of defects at the surface of silica is the use of optical or electron energy loss spectroscopies to detect the typical optical absorption bands.[44] The interaction with the metal atoms is expected to change the optical bands. DFT is not suited to study excited states, and therefore, we have computed optical transitions induced by the adsorption of a Cu atom on some dominant defects at the silica surface by means of multireference configuration interaction calculations (MRDCI). Single and double excitations from the highest occupied levels (20−30 electrons correlated) have been generated with respect to a set

(34) Becke, A. D. *J. Chem. Phys.* **1993**, *98*, 5648.
(35) Lee, C.; Yang, W.; Parr, R. G. *Phys. Rev. B* **1982**, *37*, 785.
(36) Franci, M. M.; Pietro, W. J.; Hehre, W. J.; Binkley, J. S.; Gordon, M. S.; DeFrees, D. J.; Pople, J. A. *J. Chem. Phys.* **1982**, *77*, 3654.
(37) Gordon, M. S.; Binkley, J. S.; Pople, J. A.; Pietro, W. J.; Hehre, W. J. *J. Am. Chem. Soc.* **1982**, *104*, 2797.
(38) Watchers, A. J. H. *J. Chem. Phys.* **1970**, *52*, 1033.
(39) Hay, P. J.; Wadt, W. R. *J. Chem. Phys.* **1985**, *82*, 299.
(40) Wadt, W. R.; Hay, P. J. *J. Chem. Phys.* **1985**, *82*, 284.
(41) Boys, S. F.; Bernardi, F. *Mol. Phys.* **1970**, *19*, 553.
(42) Emsley, J.; Hoyte, O. P. A.; Overill, R. E. *J. Am. Chem. Soc.* **1978**, *100*, 3303.
(43) Baerends, E. J.; Gritsenko, O. V. *J. Phys. Chem. A* **1997**, *101*, 5383.
(44) Buenker, R. J.; Peyerimhoff, S. D. *Theor. Chim. Acta* **1974**, *35*, 33.

Table 1. Absorption Properties of Cu, Pd, and Cs on Regular O Sites on the Two-Coordinated Bridging Oxygens of the Silica Surface (B3LYP BSSE-Corrected Results)

	Cu	Pd	Cs
r(M−O), Å	2.46	2.43	3.52
D_e (BSSE), eV	0.08	0.22	0.11
D_e (no BSSE), eV	0.56	0.73	0.35
spin density on M	0.94	- - -	0.97

of main (M) configurations; for further details see refs 23 and 24. The MRDCI calculations are meant specifically to deal with the problem of the clusters excited states; in principle, they could be used also to determine the importance of correlation effects on other properties such as the binding energies by determining explicitly correlated wave functions. However, the lack of analytic gradients for CI wave functions prevents us from using this technique to determine adsorption energies. The CI calculations have been performed at the HF optimal geometries. The similarity of the HF and DFT optimal geometries provides a justification for this approach. Absorption intensities have been estimated by means of the oscillator strength, *f*, a dimensionless quantity, using the dipole-length operator formula:

$$f(\mathbf{r}) = {}^2/_3|\langle\Psi_0|e\mathbf{r}|\Psi_n\rangle|^2(E_n - E_0) \qquad (1)$$

Typical values of *f* for allowed transitions are between 0.1 and 1.

The calculations have been performed using the Gaussian94 program package;[45] for the MRDCI calculations, we used the Gamess-UK code.[46]

3. Adsorption Properties of Cu, Pd, and Cs on Silica Regular and Defect Sites

3.1. Regular Sites. The interaction of the isolated Cu, Pd, and Cs atoms with the regular surface sites of silica has been modeled by the $(HO)_3Si-O-Si(OH)_3$ cluster (Figure 1a). We have considered the interaction of the metal atoms vertically above the two-coordinated bridging oxygen (Figure 1b) by keeping fixed the cluster structure. This corresponds to an "on-top" adsorption. For all three metals we found a weak interaction. At the HF level the curves are purely repulsive; at the DFT level the interaction energies are of the order of 0.3−0.7 eV, but after inclusion of the BSSE, the binding energies are extremely small, 0.1−0.2 eV (Table 1). The large BSSE is in part due to the use of contracted basis set for the core orbitals of the Si and O atoms. The potential energy curves are flat, and the equilibrium distances are rather long, in particular for Cs. This is also why the BSSE for Cs is much smaller than for Cu and Pd, Table 1. We have also performed a full geometry optimization of the metal atom position without imposing any constraint. However, given the weak nature of the interaction, this leads to spurious adsorption geometries where the adsorbate interacts with more than a surface oxygen. While this is probably what happens in reality, i.e., metal atoms interact simultaneously with two or more surface oxygens, the clusters used are too small to properly describe this bonding mode. However, the important conclusion is that the regular sites of the silica surface are very unreactive toward the metal atoms. It is worth noting that our calculations indicate for the adsorption of Pd on the O atoms of silica a bond strength which is even lower than that of the rather unreactive MgO surface.[12] This means that atoms deposited on silica from the gas phase will not be trapped at the regular sites but rather will diffuse on the surface, remain trapped at a defect, or re-evaporate.

Table 2. Absorption Properties of Cu, Pd, and Cs on the E′ Center, ≡Si•, on the SiO_2 Surface

	method	Cu	Pd	Cs
r(M−Si), Å	HF	2.365	2.362	3.553
	B3LYP	2.238	2.250	3.531
D_e (BSSE), eV	HF	1.00	1.01	0.09
D_e (BSSE), eV	B3LYP	2.32	2.27	0.88
D_e (no BSSE), eV	B3LYP	3.08	3.01	1.07
q_M	B3LYP	−0.57	−0.38	+0.45
nd	B3LYP	9.92	9.47	- - -
q_{Si}[a]	B3LYP	+1.12	+0.91	+0.39
spin density on M	B3LYP	- - -	0.88	- - -

[a] q_{Si} on the free cluster is +0.61.

3.2. Surface E′$_s$ Centers. Si sp^3 dangling bonds, ≡Si• (Figure 2a) are present on the (0001) and (1010) surfaces of α-quartz[28,30,31] and on mechanically activated silica[27] as well as on UHV-grown thin SiO_2 films.[29] The presence of these defects on the SiO_2 surface is shown by typical EPR signals, in particular by a hyperfine coupling constant of ≈470 G with the ^{29}Si nuclide[27,28] and by an intense optical transition centered around 6 eV similar to that observed in bulk silica.[27,29−31] The ≡Si• surface radical is rather reactive toward molecular species but also toward metal atoms. However, very different bonding interactions occur with different metals. Cu and Pd, in fact, form rather strong bonds with the defect site, of ≈1 eV in HF and ≈2.3 eV at the B3LYP level (BSSE-corrected values). The formation of such a strong bond is reflected in the rather short Si−M distance (M = Cu, Pd) (Figure 2b), which is almost identical for the open shell Cu or for the closed shell Pd atoms, ≈2.2 Å (Table 2). The bonding can be described as largely covalent, and the polarization of the bonding electrons is toward the metal, at least according to the Mulliken charges. For the case of Pd adsorption, the resulting spin density is almost entirely located on the metal atom.

Despite the similar structural characteristics, the bonding mechanism of Cu and Pd with ≡Si• is somewhat different. In Cu it arises from the coupling of the Si sp^3 singly occupied orbital and the metal 4s open shell orbital with formation of a σ bonding level. This orbital appears as an impurity level in the band gap of the material. Pd, on the other hand, forms a bond through a direct involvement of the 4d orbitals with the SiO_2 surface state. This implies a configuration change which increases the $4d^95s^1$ character of the metal atom (Table 2).

We consider now the bonding of a Cs atom with the same defect. In principle, one could expect for Cs a similar bonding mechanism as for Cu. At first order, this is indeed the case, although with some substantial differences. Given the large size of the Cs atom, the Si−M bond distance is very large, about 3.5 Å, and similar at the HF or B3LYP level (Table 2). The bonding, however, is almost entirely due to correlation effects. In fact, after BSSE correction, a stabilization of 0.09 eV only is found at the HF level while a D_e of 0.9 eV is found in DFT. Also the nature of the interaction is different from the Cu case. The adsorbed Cs, in fact, becomes positively charged with reduction of the net positive charge on Si, indicating the formation of a Si−Cs covalent bond strongly polarized toward Si.

The different natures of the Si−M interactions for Cu, Pd, and Cs are shown also by the analysis of the core levels of the SiO_2 substrate. We start from the discussion of the Cs adsorption case. The charge donation from the electropositive Cs atom to

(45) Frisch, M. J.; et al. *Gaussian 94*; Gaussian Inc.: Pittsburgh, PA, 1997.

(46) Guest, M. F.; Sherwood, P. *GAMESS-UK Reference Manual*; SERC, Daresbury Laboratory: Daresbury, U.K., 1992.

Table 3. Core Level Ionization Potentials (IPs) and Core Level Shifts (ΔIPs) (both in eV) for Cu, Pd, Cs, and Na Atoms Adsorbed on a E′ Center on the Silica Surface

	≡Si• or M	≡Si−Cu		≡Si−Pd		≡Si−Cs		≡Si−Na	
	IP	IP	ΔIP	IP	ΔIP	IP	ΔIP	IP	ΔIP
				HF					
O (1s)	559.7	559.3	−0.4	559.4	−0.3	557.4	−2.3	558.5	−1.2
Si (2p)	116.4	115.8	−0.6	115.9	−0.5	113.5	−2.9	114.9	−1.5
M[a]	- - -	970.0	+0.5	106.1	+3.7	34.7	+0.1	41.7	+0.2
				B3LYP					
O (1s)	517.8	517.9	+0.1	518.0	+0.2	516.0	−1.8	- - -	- - -
Si (2p)	99.8	100.0	+0.2	100.1	+0.3	97.8	−2.0	- - -	- - -
M[a]	- - -	924.9	+0.9	90.0	+2.6	28.0	−0.1	- - -	- - -

[a] The shifts have been computed with respect to the free atoms values: Cu (2p) HF = 969.5 eV, B3LYP = 924.0 eV; Pd (4s) HF = 102.4 eV, B3LYP = 87.3 eV; Cs (5s) HF = 34.6 eV, B3LYP = 28.1 eV; Na (2p) HF = 41.5 eV.

the substrate is shown by the large negative shift, to smaller binding energies, of both O (1s) and Si (2p) levels (Table 3). The shifts, 2−3 eV, are in the same direction and of similar magnitude in HF and DFT, indicating that the bonding is described in the same way by the two approaches. The large shifts on the substrate are not accompanied by a corresponding positive shift of the Cs (5s) level. In principle this could be due to the fact that the 5s is not really a core level. Indeed, in the CsCl molecule, simple HF calculations show that the core levels shift by 1.1 eV while the 5s shifts by only 0.3 eV. However, similar calculations performed on Na adsorption on the silica E′ center show the same features observed for Cs, i.e., a negative shift of the substrate core level IPs, and no shift for the Na levels (Table 3). This suggests the formation of a partial covalent bond between the metal atom and the surface Si atom which leads to the accumulation of electronic charge in the internuclear region and in the corresponding screening of the metal core hole.

When Cu and Pd are considered, we found significant differences in the behavior of the core levels. At the HF level, we observe a small negative shift of the O (1s) and Si (2p) levels, by ≈−0.5 eV, which suggests a polarization of the bonding electrons toward the silica defect, opposite to the Mulliken data. At the DFT level, however, the O (1s) and Si (2p) shifts are small but positive, ≈+0.2 eV, Table 3. This is accompanied by a moderate positive shift of the Cu (2p), +0.9 eV, and by a very large positive shift of the Pd (4s) levels, +2.6 eV. The shift of the metal core levels to higher binding energies are easily explained with a change in configuration upon adsorption which reduces the d^{10} character of the atom. The decrease of the d population results in a reduced screening of the core levels and in large upward shifts.[47] In this respect, the shifts of the adsorbed atoms are not very useful to characterize the amount of charge transfer from the adsorbate to the substrate.[48,49] The fact that the O (1s) and Si (2p) levels shift differently in HF and DFT, Table 3, is probably due to the different meaning of the eigenvalues in the two approaches but may also reflect some changes in the bonding due to correlation effects. A stronger covalent character in DFT can explain the change in the O and Si core level shifts (Table 3). In conclusion, the analysis of the substrate core levels shows that the ≡Si−M bond for Cu and Pd is largely covalent while for Cs there is an important charge transfer to the oxide. This is consistent with the net charges computed for the adsorbed metal atoms (Table 2).

To check the effect of the metal adsorption on the spectral properties of the surface, we have considered the optical transition of the $(HO)_3Si-Cu$ cluster. These have to be compared with those of the surface defect, E'_S, obtained with the same computational approach, 5.8−6.0 eV;[50] the intensity is predicted to be medium on the surface, $f(\mathbf{r}) \approx 2 \times 10^{-2}$, and strong in the bulk, $f(\mathbf{r}) \approx 2 \times 10^{-1}$.[50] The calculations shows that when the Si−Cu bond is formed the transition is shifted to 2.3 eV and the intensity of the transition decreases by 1 order of magnitude, $f(\mathbf{r}) = 5 \times 10^{-3}$. The disappearance of the typical 5.8 eV optical band, as well as of the EPR signal, should provide a clear indication of the saturation of the surface dangling bonds upon metal adsorption.

3.3. Nonbridging Oxygens. Nonbridging oxygens at the surface of silica, ≡Si−O• (Figures 3a and 4a), represent probably the most important defects for the reactivity of mechanically activated SiO_2. These broken bonds have been proposed as the centers where impinging Cu atoms are trapped from metastable impact electron spectroscopy experiments (MIES).[22] The fingerprint of their existence is given by a characteristic doublet in the EPR signal and by an hyperfine splitting with the ^{17}O nuclide as well as by an optical absorption band at about 2 eV;[25−27] this absorption band, however, is rather weak in glassy silica, $f(\mathbf{r}) \approx 10^{-4}$, and may be difficult to detect at the SiO_2 surface.

All three metal atoms considered, Cu, Pd, and Cs, form strong bonds with the NBO centers (Tables 4 and 5). Using a minimum 1-T model of the surface defect (Figure 3b), the computed BSSE-corrected D_e values at the B3LYP level are 3.13, 2.51, and 2.99 eV for Cu, Pd and Cs, respectively, i.e., considerably stronger than the corresponding bonds formed with the surface E'_S centers. These values increase when a larger model of the surface is used (Figures 4b,c and Table 5). In this case, in fact, the D_e values are 3.79, 2.85, and 3.51 for Cu, Pd, and Cs, respectively. The reason for the different response of the two surface models is not a strong cluster-size dependence of the adsorption properties, but rather is a direct consequence of the ≡Si−O−M bonding nature. The metal atoms directly bound to the surface oxygen, in fact, become partially oxidized, although to a different extent. Cs donates almost an entire electron to the SiO_2 substrate and becomes Cs^+; Cu and Pd form bonds with more covalent character with the ≡Si−O• group, but with an important polarization toward oxygen (partial charge transfer). A net residual positive charge forms also on adsorbed Cu and Pd atoms. This is shown by the data of the Mulliken population (Tables 4 and 5) and can be seen from the analysis of the core levels (see below).

(47) Bagus, P. S.; Brundle, C. R.; Pacchioni, G.; Parmigiani, F. *Surf. Sci. Rep.* **1993**, *19*, 265.
(48) Bagus, P. S.; Pacchioni, G. *Phys. Rev. B* **1993**, *48*, 15262.
(49) Clotet, A.; Ricart, J. M.; Illas, F. *Surf. Sci.* **1996**, *364*, 89.
(50) Pacchioni, G.; Ieranò, G.; Marquez, A. *Phys. Rev. Lett.* **1998**, *81*, 377.

Table 4. Absorption Properties of Cu, Pd, and Cs on the NBO Center, ≡Si−O•, on the SiO_2 Surface (One-Tetrahedron Model, Figure 3b)

	method	Cu	Pd	Cs
r(M−O_1), Å	HF	1.994	2.138	2.820
	B3LYP	1.941	2.093	2.807
r(M−O_2), Å	HF	2.105	2.295	3.020
	B3LYP	2.037	2.232	3.005
r(Si−O_1), Å	HF	1.574	1.576	1.553
	B3LYP	1.607	1.614	1.573
r(Si−O_2), Å	HF	1.730	1.723	1.717
	B3LYP	1.747	1.736	1.733
α(M−O_1−Si), deg	HF	97.1	99.9	106.4
	B3LYP	93.6	97.2	105.7
D_e (BSSE), eV	HF	2.10	1.87	1.95
D_e (BSSE), eV	B3LYP	3.13	2.51	2.99
D_e (no BSSE), eV	B3LYP	3.74	3.10	3.15
q_M	B3LYP	+0.25	+0.25	+0.84
nd	B3LYP	9.95	9.18	- - -
q_O[a]	B3LYP	−0.67	−0.67	−1.06
spin density on M	B3LYP	- - -	0.75	- - -

[a] q_O on the free cluster is −0.35.

Table 5. Absorption Properties of Cu, Pd, and Cs on the NBO Center, ≡Si−O•, on the SiO_2 Surface (Two-Tetrahedra Model, Figure 4b,c)

	method	Cu	Pd	Cs
r(M−O_1), Å	HF	1.944	2.116	2.849
	B3LYP	1.855	2.025	2.841
r(M−O_2), Å	HF	2.058	2.428	3.255[a]
	B3LYP	1.930	2.203	3.181[a]
r(Si−O_1), Å	HF	1.578	1.579	1.547
	B3LYP	1.622	1.611	1.570
r(Si−O_2), Å	HF	1.724	1.714	1.687[a]
	B3LYP	1.764	1.745	1.718[a]
α(M−O_1−Si), deg	HF	108.1	118.2	123.0
	B3LYP	96.3	114.8	125.0
D_e (BSSE), eV	HF	2.56	2.19	2.58
D_e (BSSE), eV	B3LYP	3.79	2.85	3.51
D_e (no BSSE), eV	B3LYP	4.93	3.74	3.78
q_M	B3LYP	0.00	+0.17	+0.82
q_O[b]	B3LYP	−0.69	−0.68	−0.84
spin density on M	B3LYP	- - -	0.79	- - -

[a] Average value, see Figure 4b. [b] q_O on the free cluster is −0.39.

The fact that the metal atoms becomes partially (Cu and Pd) or fully (Cs) ionized leads to important interactions with the neighboring surface O atoms. The adsorbate interacts, mostly electrostatically, with the exposed two-coordinated O atoms of the surface which become effectively three-coordinated. This results in the formation of rings where the metal atom binds to two (Cu, Pd) (Figure 4b) or even three (Cs) surface oxygens (see Figure 4c). The distance of the metal atom from the other surface oxygens is somewhat larger than that from the NBO (see Table 5); this can be interpreted as due to the existence of a direct covalent interaction between the metal and O_1, even for the almost fully ionized Cs atom. Clearly, a small cluster which does not contain neighboring tetrahedra does not allow for the formation of these six-member rings (Figure 4b) or more complex structures (Figure 4c) and results in a smaller binding energy. This is clearly shown in Figure 3b, where the formation of strained four-member rings is apparent. It is interesting to mention that the formation of six-member rings similar to those shown in Figure 4b has recently been demonstrated from XAFS measurements on the deposition of Ni^{2+} ions on amorphous silica.[4] The formation of "three-coordinated" oxygens on the surface bonded simultaneously to two Si and one metal atoms is not merely an artifact due to the use of small clusters (in our models the three-coordinated oxygen is indeed bonded to a saturating H atom and not to a SiO_4 tetrahedron); in fact, calculations performed using larger clusters and 6-31G* basis sets on all oxygens also show the formation of six-membered "rings".

The analysis of the core levels (Table 6) helps in characterizing the bonding. At the HF level, the O (1s) orbital of the NBO is shifted to smaller binding energies by 3.8 eV for Cu and Pd adsorption, by 4.8 eV for Na (considered for comparison), and by 6.2 eV for Cs. This is consistent with a large charge transfer from the metal to the surface oxygen which follows the trend Cs > Na > Cu ≈ Pd. The negative shift of the O (1s) is found also at the DFT level, although less than in HF (Table 6). This may indicate a more covalent interaction in DFT, or it could simply due to final state relaxation effects. Still, the shifts are large. Negative shifts are found in HF also for the Si (2p) core levels, by 3.3 eV for Cs, 2.1 eV for Na, and 1.5 eV for Cu and Pd. The DFT shifts are smaller but follow exactly the same trend (Table 6). This provides strong evidence of the increased charge density on the SiO_2 surface due to charge flow from the adsorbed metal. Negative shifts occur also for the (1s) level of the three-coordinated oxygen "electrostatically" bound to the metal. These shifts are much smaller than for the NBO and may reflect the penetration of the metal charge density into the surface charge distribution with increased Pauli repulsion and destabilization of the oxygen core levels. The core levels of the adsorbed metal atom are much less indicative of the nature of the interaction because of the mixing with other important effects which contribute to the final shift. The first of these effects is the already mentioned s−d hybridization which reduces the d population,[47] particularly important for Pd which goes from a d^{10} configuration in the free atom to a nearly d^9 configuration on the surface (Table 4). Thus, as shown for other adsorbates and substrates,[48,49] the shift of the adsorbed metal core levels is not very indicative of the nature of the interaction.

The formation of the ≡Si−O−M bond has important consequences also on the transition energies. We have analyzed this for the case of Cu. Since the bonding of the open shell NBO and Cu fragments leads to a closed shell system, it is not surprising that the typical transition of the NBO, centered at 2.0 eV and computed at 2.2 eV,[25] disappears and is replaced by a much higher transition around 7 eV with a modest intensity, $f(\mathbf{r}) \approx 2 \times 10^{-2}$. A feature of this kind will be probably covered by the tails of other absorption bands (in particular, oxygen vacancies and silanol groups) and could be hard to detect.

3.4. Neutral Oxygen Vacancy. Neutral oxygen vacancies, V_O, are quite abundant in glassy silica or in irradiated α-quartz.[26] The defects arise from the recombination of two ≡Si• dangling bonds derived from the removal of a neutral oxygen, ≡Si−Si≡ (Figure 5a). As a consequence, the Si−Si distance, which in nondefective silica is of 3.06 Å, in a V_O center becomes ≈2.5 Å.[24] This defect is diamagnetic, and its presence can be detected only from optical absorption and photoluminescence measurements. Indeed, a typical OA band around 7.6 eV with strong intensity has been unambiguously assigned to the V_O defect.[24] The presence of the V_O centers at the (1010) surface of α-quartz or in SiO_2 thin films is clearly shown by the EELS spectra exhibiting a prominent feature at 7.2−7.5 eV.[29−31] It can be expected that this diamagnetic defect will be less reactive toward metal atoms than the paramagnetic E_S' and NBO centers. Using the $(HO)_3Si-Si(OH)_3$ model of a V_O defect we have considered the adsorption properties of Cu, Pd, and Cs atoms (Table 7).

We have to mention that, given the strong relaxation following the interaction with the metal atom, a precise estimate of the BSSE is not possible. The BSSE has been evaluated as

Table 6. Core Level Ionization Potentials (IPs) and Core Level Shifts (ΔIPs) (both in eV) for Cu, Pd, Cs, and Na Atoms Adsorbed on a Nonbridging Oxygen on the Silica Surface (1-T Model, Figure 3)

	≡Si−O• or M	≡Si−O−Cu		≡Si−O−Pd		≡Si−O−Cs		≡Si−O−Na	
	IP	IP	ΔIP	IP	ΔIP	IP	ΔIP	IP	ΔIP
				HF					
O_1 (1s)	560.2	556.4	−3.8	556.4	−3.8	554.0	−6.2	555.4	−4.8
O_2 (1s)	560.1	559.5	−0.6	559.4	−0.7	557.8	−2.3	558.9	−1.2
Si (2p)	117.0	115.6	−1.5	115.5	−1.5	113.7	−3.3	114.9	−2.1
M[a]	- - -	969.4	−0.2	106.6	+4.2	34.0	−0.5	40.8	−0.7
				B3LYP					
O_1 (1s)	521.7	519.0	−2.7	519.4	−2.3	516.2	−5.5	- - -	- - -
O_2 (1s)	518.3	518.0	−0.3	518.8	+0.5	515.9	−2.4	- - -	- - -
Si (2p)	100.7	99.9	−0.8	100.1	−0.6	97.7	−3.0	- - -	- - -
M[a]	- - -	924.1	+0.1	90.4	+2.9	27.7	−0.4	- - -	- - -

[a] The shifts have been computed with respect to the free atoms values: Cu (2p) HF = 969.5 eV, B3LYP = 924.0 eV; Pd (4s) HF = 102.4 eV, B3LYP = 87.3 eV; Cs (5s) HF = 34.6 eV, B3LYP = 28.1 eV; Na (2p) HF = 41.5 eV.

Table 7. Absorption Properties of Cu and Pd on the Neutral Oxygen Vacancy, ≡Si−Si≡, on the SiO_2 Surface

	method	Cu	Pd
r(M−Si_1), Å	HF	2.335	2.306
	B3LYP	2.272	2.275
r(M−Si_2), Å	HF	2.439	2.309
	B3LYP	2.282	2.278
r(Si−Si), Å	HF	3.878	3.294
	B3LYP	4.057	3.471
α(Si−M−Si), deg	HF	108.6	91.3
	B3LYP	125.9	99.3
D_e (BSSE), eV	HF	unbound	0.21
D_e (BSSE), eV	B3LYP	0.55	2.16
D_e (no BSSE), eV	B3LYP	1.99	3.53
q_M	B3LYP	−1.07	−0.89
nd	B3LYP	9.88	9.39
q_{Si}[a]	B3LYP	+1.05	+0.97
spin density on M	B3LYP	0.43	- - -

[a] q_{Si} on the free cluster is +0.70.

described in section 2, but the correction is largely overestimated. In the following we discuss mostly the BSSE-corrected results, but it should be kept in mind that these represent only lower bounds to the actual interaction energy. Noncorrected values are given in Table 7.

The behaviors of the three metal atoms are very different. At the HF level, and without BSSE corrections, Cs is unbound, Pd is bound by 1.20 eV and Cu is trapped in a local minimum which lies 0.2 eV above the dissociation limit. At the DFT level, Pd and Cu are bound, by 2.16 and 0.55 eV, respectively, after BSSE; Cs is very weakly bound, 0.13 eV with BSSE, 0.35 eV without, and the bond arises entirely from dispersion forces. Thus, while the TM atoms form strong bonds with the Si atoms of the surface, Cs does not react at all with this defect. The main reason for the different behavior lies, besides the different electronic structure, in the atomic size. In fact, the bonding interaction of the ≡Si−Si≡ defect with the metal atom results in a ≡Si−M−Si≡ structure where M replaces the missing O atom of the nondefective surface (Figure 5b). This leads to a strong geometrical relaxation and in particular to a considerable increase of the Si−Si distance which goes from ≈2.5 Å to ≈4 Å (Cu) and ≈3.5 Å (Pd) (Table 7). The presence of a singly occupied diffuse 5s orbital is the reason for the larger distortion of the lattice and of the weaker bonding in the Cu case (Table 7). The inclusion of Cs in the Si−Si bond would probably require an even higher relaxation, but this would result in very strained structure. As a consequence, only a very shallow minimum is found for Cs at about 4.3 Å from the Si atoms which retain the Si−Si distance of the free surface defect, 2.49 Å.

Table 8. Core Level Ionization Potentials (IPs) and Core Level Shifts (ΔIPs) (both in eV) for Cu, Pd, Cs, and Na Atoms Adsorbed on a Oxygen Vacancy on the Silica Surface

	≡Si−Si≡ or M	≡Si−Cu−Si≡		≡Si−Pd−Si≡	
	IP	IP	ΔIP	IP	ΔIP
		HF			
O (1s)	559.3	560.0	+0.7	559.8	+0.5
Si (2p)	116.5	116.5	0.0	116.6	+0.1
M[a]	- - -	970.5	+1.0	105.7	+3.3
		B3LYP			
O (1s)	517.2	518.2	+1.0	518.0	+0.8
Si (2p)	99.8	100.2	+0.3	100.2	+0.4
M[a]	- - -	925.9	+1.9	90.4	+3.1

[a] The shifts have been computed with respect to the free atoms values: Cu (2p) HF = 969.5 eV, B3LYP = 924.0 eV; Pd (4s) HF = 102.4 eV, B3LYP = 87.3 eV.

When Cu and Pd are bound to the ≡Si−Si≡ defect, relatively short Si−Cu and Si−Pd distances result, ≈2.3 Å at the B3LYP level (Table 7). In Cu, the unpaired electron of the structure is localized for only 40% on the metal atom, the rest being delocalized over the Si−Cu−Si network. The bonding of Cu and Pd with the Si atoms is of largely covalent nature, but the Mulliken charges show a decrease of electronic charge on Si and an accumulation of charge on the metal.

The analysis of the core levels (Table 8) shows a moderate increase of the (1s) IP of the O atoms next-neighbors to the adsorbed metal, at both HF and DFT levels. Small positive shifts are found also for the Si (2p) levels. This is consistent with the data of the Mulliken population which suggests a flow of charge from the $(-O)_3Si$ units to the adsorbed metal. The accumulation of negative charge on M indicated by the Mulliken (Table 7) is not accompanied by a corresponding negative shift of the metal core or semicore levels (Table 8) because, as discussed before, of the canceling effect of the s−d hybridization. Indeed, the Mulliken analysis shows that Cu and Pd have d populations of ≈9.9 and ≈9.4 electrons, respectively (Table 7).

As we mentioned in the Introduction, the fingerprint of the existence of oxygen vacancies in SiO_2 bulk and surface is given by a typical absorption band at 7.6 eV.[24,26] The interaction with metal atoms is expected to change and eventually remove this band. We have considered this effect for the case of Cu by computing the lowest doublet-to-doublet transitions for a $(HO)_3Si-Cu-Si-(OH)_3$ cluster. We found two transitions, at 0.9 and 2.1 eV, with very low intensity, $f(\mathbf{r}) \approx 10^{-4}$. This is a clear indication that upon metal deposition the 7.6 eV band will disappear without being replaced by similar intense features in the same spectral region.

Table 9. Valence Levels of Nondefective and Defective Silica and of Cs Atoms Adsorbed at Silica Defects

	regular SiO_2		NBO	E′	NBO/Cs	E′/Cs
system	≡Si−O−Si≡	O (2p)	≡Si−O•	≡Si•	≡Si−O−Cs	≡Si−Cs
theory[a]	≈12−13	≈7.5	≈8	≈5	≈4.5	≈3
expt[b]	10.7−11.3	7.8	not seen	not seen	6.0	not seen

[a] The features are derived from the Kohn−Sham eigenvalues and are computed with respect to the vacuum level taken as reference. [b] The experimental values, ref 22, are referred to the Fermi level.

4. Discussion and Conclusions

The results presented in the previous session allow us to draw some general conclusions about the interaction mode of metal atoms on the dehydroxilated silica surface. First of all, there is a clear indication that the two-coordinated bridging oxygens of the surface, ≡Si−O−Si≡, are very unreactive. Only weak, dispersion interactions occur between the metal and these sites. This means that the atoms adsorbed from the gas phase will rapidly diffuse on the surface without being trapped except at defect sites. Therefore, these are the sites where clustering and metal aggregation processes are likely to begin. These results are fully consistent with measurements of the sticking coefficient of Cu on SiO_2. Zhou et al. found that at 300 K only one-third of the initially incident Cu atoms stick to the surface;[20] Xu and Goodman found that the sticking depends markedly on the temperature, varying from 0.6 at 90 K to 0.1 at 400 K.[18] Both studies agree with the fact that the bonding of Cu with the clean surface is weak and that sticking occurs only at the defect sites. The very weak interaction with the substrate is the reason for the Volmer−Weber growth mode of metal overlayers on silica with formation of 3D clusters and small metal particles.[51,52] Experimentally, it has not been possible so far to identify which are the defects responsible for the sticking. We have found that, among the three major defect sites considered, the nonbridging oxygen, ≡Si−O•, is the most reactive followed by the surface E'_S centers, ≡Si•, and by the neutral oxygen vacancies, ≡Si−Si≡. All these defects form strong bonds with Cu, Pd, and Cs metal atoms. The only exception is the neutral vacancy which does not react with Cs. The deposition of Cu below 0.1 monolayer coverage results in a 0.6 shift of the Cu 2p core levels to higher binding energies, suggesting partial oxidation of the metal overlayer.[19] Our results show that the core level shifts of an isolated transition metal atom are not easy to interpret because of the large contributions from the s−d hybridization. For the three defects considered we found shifts of the Cu 2p levels which range from +0.2 to +1.9 eV. While this is in broad agreement with the experiment,[19] it does not allow for a clear identification of the defects which are responsible for the sticking of the Cu atoms.

The formation of the new surface species, ≡Si−O−M, ≡Si−M, or ≡Si−M−Si≡, results in characteristic features in the band gap of the material associated to the bonding levels formed between the surface defect and the metal atom. Some of these features have been recently measured by MIES and UPS experiments for the case of Cs adsorption on silica.[22] The silica substrate has been prepared from natural oxidation of Si(100) and further exposure of the thin oxide film to oxygen at room temperature. The MIES and UPS spectra of the clean surface show two peaks at 7.8 and ≈11 eV assigned to the nonbonding O (2p) and to the σ-type Si−O−Si bonding levels of the silica surface;[22] the features have been measured with respect to the Fermi level. To better understand these features we have considered the one-electron energies of our clusters. The following discussion, based on the Kohn−Sham eigenvalues, is purely qualitative. Taking the $(HO)_3Si-O-Si(OH)_3$ cluster as a model of the surface, we found an HOMO−LUMO gap at the DFT level of 8.3 eV; the experimental gap on silica surface is of ≈8.6−8.8 eV.[30,31] The top of the O (2p) "valence band" in our cluster is ≈8 eV below the vacuum level. We take this level as our reference energy. The group of Si−O bonding levels is centered around 12−13 eV, ≈4−5 eV below the O (2p) band, similar to the experiment (Table 9). If we consider now the cluster models of the defect centers, in particular the NBO site, ≡Si−O•, we have a clear indication that this group does not give rise to a specific feature in the band gap but its valence levels are embodied in the O (2p) band (Table 9). This means that, even if these defects are present on the surface at sufficiently high concentration, they will not be detected by MIES or UPS experiments. Similarly, also a surface peroxo radical, ≡Si−O−O•, shows O (2p) features at the same energy as the regular surface. The E′ center, ≡Si•, on the other hand, should result in a typical feature in the band gap (about 5 eV below the vacuum level according to our estimates) and should result in a separated peak in the experiment. The fact that this peak is not seen could indicate that a very small concentration of these sites is present on the surface. This is not surprising if we consider that the surface was exposed to 500 L of oxygen at room temperature.[22] It is very likely that in these conditions the following reactions take place:

$$\equiv Si^{\bullet} + O_2 \rightarrow \equiv Si-O-O^{\bullet} \quad (2)$$

$$\equiv Si^{\bullet} + O_2 \rightarrow \equiv Si-O^{\bullet} + O(^3P) \quad (3)$$

$$2(\equiv Si^{\bullet}) + O_2 \rightarrow 2(\equiv Si-O^{\bullet}) \quad (4)$$

Reaction 2 occurs with an energy gain of 2.8 eV, while reaction 3 is endothermic by 0.1 eV only (B3LYP results), indicating that in principle ≡Si• groups can activate the O_2 dissociation; reaction 4 is very exothermic, by 5.2 eV. Therefore, a great concentration of NBO or peroxy radical centers is expected on the surface after exposure to O_2.

Upon adsorption of Cs, new features appear in the MIES and UPS experimental spectrum at 3.5 and 6 eV below the Fermi level.[22] These features have been assigned to the formation of new surface bonds, ≡Si−O−Cs, 6-eV feature, and to the presence of molecular oxygen or peroxo species, 3.5-eV band.[22] In our calculations, the formation of the ≡Si−O−Cs bond is accompanied by the appearance of a corresponding level at ≈4.4 eV, i.e., about 3 eV above the top of the O (2p) band. This is close enough to the observed 6-eV peak, i.e., 1.8 eV above the O (2p) feature, to suggest that this is indeed the origin of the observed peak. A ≡Si−Cs bond resulting from the interaction of the Cs atom with the E′ centers, on the other hand, should result in a new feature at about 3 eV, i.e., well above the top of the valence band. This peak has not been observed consistent with the idea that only few E′ centers are present on the surface after exposure to oxygen. This discussion provides strong support to the hypothesis that the most reactive centers at silica

(51) Bellamy, B.; Mechken, S.; Masson, A. *Z. Phys. D* **1993**, *26*, 61.
(52) Xu, X.; Goodman, D. W. *J. Phys. Chem.* **1993**, *97*, 683.

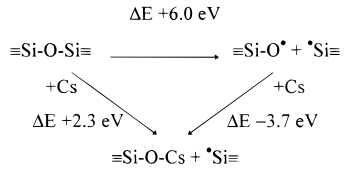

Figure 6. Energetics of the insertion of a Cs atom into a ≡Si−O−Si≡ bond (B3LYP values). Negative Δ*E* values indicate exothermicity.

surfaces prepared by silicon oxidation are the nonbridging oxygens. This is true not only for Cs adsorption but also for other metals such as Cu, as recently suggested by Goodman and co-workers.[19]

An important question is whether the NBO centers are preexisting, i.e., are present before the exposure to the metal, or if they form during the metal deposition at the expenses of the ≡Si−O−Si≡ siloxane groups:

$$\equiv Si-O-Si\equiv + M \rightarrow \equiv Si-O\text{-}M + {}^{\bullet}Si\equiv \quad (5)$$

$$\equiv Si-O-Si\equiv + M \rightarrow \equiv Si-O^{\bullet} + M\text{-}Si\equiv \quad (6)$$

To answer this question we have considered the energetics of the two processes for the case of Cs (Figure 6). Extension to the other metal atoms considered is rather straightforward using the D_e values of Tables 2 and 4 and led to the same general conclusion. Reactions 5 and 6 imply the breaking of a Si−O bond compensated by the formation of a Si−O−M or of a direct Si−M bond. The results presented in the previous sections clearly show that the Si−O−M bond is preferred over that Si−M one. However, gradient-corrected DFT calculations (Figure 6) indicate that the energy required to break the Si−O bond, about 6 eV, is not compensated by the formation of a metal−oxygen bond. This is true not only for Cs but also for the other metals considered. Therefore, it is unlikely that Si−O−M surface bonds will be formed at the expenses of the siloxane bond, unless very strained ≡Si−O−Si≡ groups are present on the surface as suggested by molecular dynamics simulations.[53] However, no experimental proof that the strained groups actually exist has been reported so far.

A final comment is related to the optical and EPR properties of a metal-covered silica surface compared to the free substrate. It has been shown that typical optical bands at 5.8 and 7.6 eV are present on the surface of quartz and SiO_2 thin films.[26−31] These features are associated to the presence of defects at the surface. The interaction and bond formation with the metal atoms results in dramatic changes in the optical properties of the surface and, in particular, in the removal of the prominent bands seen on the "clean" surface. Thus, deep changes in the electronic excitations of a silica surface after metal deposition are predicted on the basis of the present calculations. In particular, the pronounced, intense bands associated to some typical defects of amorphous silica will disappear, providing a clear indication of the formation of the metal/oxide interface. In a similar way, completely different EPR spectra will arise from low doses of metal deposition. When open shell atoms such as Cs or Cu are impinging on the surface, it is expected that the more reactive paramagnetic centers will become saturated and consequently EPR silent.

Acknowledgment. N.L. is grateful to the "Direcciò General de Recerca Generalitat de Catalunya" for supporting her visit to the Univeristy of Milano. G.P. thanks the University of Barcelona for an invited professor position. Financial support from Spanish CICyT Project No. PB95-0847-C02-01 and NATO Collaborative Research Grant No. 941191 is acknowledged. Finally, we thank the Supercomputational Center of Catalunya (CESCA) for providing part of the computer time.

JA981753C

(53) Garofalini, S. H. *J. Chem. Phys.* **1983**, *78*, 2069.